Automatic covariance pattern analysis outperforms visual reading of 18 F fluorodeoxyglucose positron emission tomography (FDG PET) in variant progressive supranuclear palsy

Ralph Buchert, Florian Wegner, Hans Jürgen Huppertz, Georg Berding, Matthias Brendel, Ivayla Apostolova, Carsten Buhmann, Alexander Dierks, Sabrina Katzdobler, Martin Klietz, Johannes Levin, Nima Mahmoudi, Andreas Rinscheid, Sophia Rogozinski, Jost Julian Rumpf, Christine Schneider, Sophia Stöcklein, Phoebe G. Spetsieris, David Eidelberg, Mike P. Wattjes, Osama Sabri, Henryk Barthel, Günter Höglinger

Automatic covariance pattern analysis outperforms visual reading of ^{18}F-fluorodeoxyglucose-positron emission tomography (FDG-PET) in variant progressive supranuclear palsy

Ralph Buchert, PhD,[1*] Florian Wegner, MD,[2] Hans-Jürgen Huppertz, MD,[3] Georg Berding, MD,[4]
Matthias Brendel, MD,[5,6,7] Ivayla Apostolova, MD,[1] Carsten Buhmann, MD,[8] Alexander Dierks, MD,[9]
Sabrina Katzdobler, MD,[6,7,10] Martin Klietz, MD,[2] Johannes Levin, MD,[6,7,10] Nima Mahmoudi, MD,[11]
Andreas Rinscheid, PhD,[12] Sophia Rogozinski, MD,[2] Jost-Julian Rumpf, MD,[13] Christine Schneider, MD,[14]
Sophia Stöcklein, MD,[15] Phoebe G. Spetsieris, PhD,[16] David Eidelberg, MD,[16] Mike P. Wattjes, MD, PhD,[11]
Osama Sabri, MD,[17] Henryk Barthel, MD,[17] Günter Höglinger, MD,[2,6,10]
for the Alzheimer's Disease Neuroimaging Initiative

[1]Department of Diagnostic and Interventional Radiology and Nuclear Medicine, University Medical
Center Hamburg-Eppendorf, Hamburg, Germany
[2]Department of Neurology, Hannover Medical School, Hannover, Germany
[3]Swiss Epilepsy Center, Zurich, Switzerland
[4]Department of Nuclear Medicine, Hannover Medical School, Hannover, Germany
[5]Department of Nuclear Medicine, University Hospital of Munich, LMU, Munich, Germany
[6]German Center for Neurodegenerative Diseases (DZNE) Munich, Munich, Germany
[7]Munich Cluster for Systems Neurology (SyNergy), Munich, Germany
[8]Department of Neurology, University Medical Center Hamburg-Eppendorf, Hamburg, Germany
[9]Department of Nuclear Medicine, University Hospital Augsburg, Augsburg, Germany
[10]Department of Neurology, University Hospital of Munich, LMU, Munich, Germany
[11]Department of Diagnostic and Interventional Neuroradiology, Hannover Medical School, Hannover, Germany
[12]Medical Physics and Radiation Protection, University Hospital Augsburg, Augsburg, Germany
[13]Department of Neurology, University of Leipzig, Leipzig, Germany
[14]Department of Neurology and Clinical Neurophysiology, University Hospital Augsburg, Augsburg, Germany
[15]Department of Radiology, University Hospital of Munich, LMU, Munich, Germany
[16]The Feinstein Institutes for Medical Research Manhasset, Manhasset, New York, USA
[17]Department of Nuclear Medicine, University Hospital of Leipzig, Leipzig, Germany

---

*Correspondence to: Dr. R. Buchert, Department of Diagnostic and Interventional Radiology and Nuclear Medicine, University Medical Center Hamburg-Eppendorf, Martinistr. 52, 20246 Hamburg, Germany; E-mail: r.buchert@uke.de

ABSTRACT: Background: To date, studies on positron emission tomography (PET) with ^{18}F-fluorodeoxyglucose (FDG) in progressive supranuclear palsy (PSP) usually included PSP cohorts overrepresenting patients with Richardson's syndrome (PSP-RS).
Objectives: To evaluate FDG-PET in a patient sample representing the broad phenotypic PSP spectrum typically encountered in routine clinical practice.
Methods: This retrospective, multicenter study included 41 PSP patients, 21 (51%) with RS and 20 (49%) with non-RS variants of PSP (vPSP), and 46 age-matched healthy controls. Two state-of-the art methods for the interpretation of FDG-PET were compared: visual analysis supported by voxel-based statistical testing (five readers) and automatic covariance pattern analysis using a predefined PSP-related pattern.
Results: Sensitivity and specificity of the majority visual read for the detection of PSP in the whole cohort were 74% and 72%, respectively. The percentage of false-negative cases was 10% in the PSP-RS subsample and 43% in the vPSP subsample. Automatic covariance pat-

tern analysis provided sensitivity and specificity of 93% and 83% in the whole cohort. The percentage of false-negative cases was 0% in the PSP-RS subsample and 15% in the vPSP subsample.
Conclusions: Visual interpretation of FDG-PET supported by voxel-based testing provides good accuracy for the detection of PSP-RS, but only fair sensitivity for vPSP. Automatic covariance pattern analysis outperforms visual interpretation in the detection of PSP-RS, provides clinically useful sensitivity for vPSP, and reduces the rate of false-positive findings. Thus, pattern expression analysis is clinically useful to complement visual reading and voxel-based testing of FDG-PET in suspected PSP. © 2023 The Authors. *Movement Disorders* published by Wiley Periodicals LLC on behalf of International Parkinson and Movement Disorder Society.

Key Words: progressive supranuclear palsy; positron emission tomography; ^{18}F-fluorodeoxyglucose; between-reader agreement; covariance pattern analysis

Progressive supranuclear palsy (PSP) is a primary four-repeat tauopathy defined neuropathologically.[1,2] Initial criteria for the ante-mortem diagnosis of PSP including the criteria of the National Institute of Neurological Disorders and Stroke Society (NINDS)[3] focus on "classical" PSP with Richardson's syndrome (RS) and, therefore, provide high specificity but only limited sensitivity, particularly at early disease stages.[4] This is related to the fact that PSP can present with various clinical phenotypes other than RS,[5] and that the phenotypic spectrum typically encountered in clinical routine is rather broad.[6]

In order to facilitate an accurate clinical diagnosis of PSP for research and clinical purposes, the PSP study group of the International Parkinson and Movement Disorder Society (MDS) proposed revised diagnostic criteria explicitly taking into account a range of different (non-RS) variant PSP (vPSP) phenotypes including "cortical" vPSP predominance types[7] such as PSP with

predominant corticobasal syndrome (PSP-CBS) and PSP with predominant frontal presentation (PSP-F) as well as "subcortical" vPSP predominance types such as PSP with predominant parkinsonism (PSP-P) and PSP with progressive gait freezing (PSP-PGF).[5] Nevertheless, additional diagnostic tests are still needed to support the diagnosis of PSP in uncertain cases in clinical routine, particularly in vPSP, as well as in clinical trial settings.[8-10]

Additional tests to support the PSP diagnosis include positron emission tomography (PET) of the brain with ^{18}F-fluorodeoxyglucose (FDG) to detect (or exclude) PSP-related metabolic abnormalities,[10-13] which have been incorporated as "supportive imaging findings" in the MDS PSP criteria.[5] Given that FDG-uptake in the brain is mainly driven by signaling-related synaptic activity,[14] brain FDG-PET is sensitive to both neuronal degeneration (at advanced disease stages) and neuronal dysfunction (at early stages).

The characteristic FDG-PET finding in PSP is reduced FDG-uptake in the bilateral frontal cortex (first described about 35 years ago)[15-21] including anterior and mid cingulate gyri, supplementary motor area, ventro- and dorsolateral premotor areas, prefrontal areas, anterior insular cortex, as well as in the striatum (most pronounced in caudate nucleus), thalamus, and midbrain ("pimple sign"[22]).[11,12,23-25] These metabolic alterations were confirmed in autopsy-proven PSP.[26-28]

The majority of previous studies on FDG-PET in PSP enrolled patients according to the NINDS criteria, including recent studies published after the release of the revised MDS criteria.[29-32] Furthermore, most of these studies selected predominantly patients with "probable" PSP to increase the accuracy of the gold standard in the absence of post-mortem verification. As a consequence, the majority of previous studies most likely included skewed PSP cohorts (overrepresenting PSP-RS compared to other predominance types) not reflecting the heterogeneity of PSP observed in clinical practice.[6,26,33] This questions the transferability of previously reported performance estimates for brain FDG-PET in the detection of PSP to clinical practice with a broad phenotypic PSP spectrum, given that reduction of FDG-uptake in vPSP predominance types might be less severe and restricted to parts of the typical PSP-RS pattern ("incomplete patterns").[26,34-38] Furthermore, many previous studies reported findings from single-site/single-scanner data that may not generalize to more general clinical settings.

The aim of this multicenter study was to evaluate brain FDG-PET for the detection of PSP in a patient sample representative of the broad phenotypic spectrum typically encountered in routine clinical practice. Two state-of-the art methods for the interpretation of FDG-PET were compared: (i) visual analysis by experienced readers supported by voxel-based statistical testing and (ii) automatic covariance pattern analysis. The following hypotheses were tested: (H1) visual analysis of FDG-PET is less sensitive for the detection of PSP in vPSP compared to PSP-RS and (H2) covariance pattern analysis outperforms visual analysis, particularly in vPSP predominance types.

Methods

Subjects

The study was designed as a phase 2 study ("ability to discriminate patients from controls") according to a five-phase framework for biomarker validation[39] and, therefore, included well-characterized patients with established PSP diagnosis and healthy controls.

Forty-one patients fulfilling the MDS PSP diagnostic criteria were included retrospectively at the University Hospitals of Augsburg (n = 1), Hamburg (n = 9),

Hannover (n = 17), Leipzig (n = 5), and Munich (n = 9). None of the patients had clinically relevant comorbidity on brain MRI such as large vessel disease, severe small vessel disease (Fazekas grade 3[40]), or mass lesions. Median and interquartile range of the delay between the date of the clinical diagnosis and FDG-PET were 0 days and −6 days to 6 days, respectively (range −210 to 441 days).

In addition, brain FDG-PET images of 46 healthy control (HC) subjects from the Alzheimer's Disease Neuroimaging Initiative (ADNI) were included. All HC subjects had been cognitively stable for ≥36 months after FDG-PET. The ADNI was launched in 2003 as a public–private partnership, led by Principal Investigator Michael W. Weiner, MD. For up-to-date information see www.adni-info.org.

Demographical and clinical characteristics are summarized in Table 1.

Image preprocessing

In the PSP patients, brain FDG-PET was performed with six different PET systems (five PET/CT, one PET/MRI) after intravenous injection of 202 ± 37 MBq FDG (range 128–317 MBq) according to the standard operating procedure at each site. The PET images were harmonized with respect to spatial resolution based on measurements of a Hoffman 3D brain phantom[44] as described in the Supplementary Material and Supplementary Figure S1 in Appendix S1.

PET images with harmonized spatial resolution were stereotactically normalized (including warping) to the anatomical reference space of the Montreal Neurological Institute using the Statistical Parametric Mapping (SPM) software package[45] with default parameter settings. For intensity scaling, each stereotactically normalized image was divided voxel-by-voxel by the individual mean intensity in brain parenchyma.[46]

Single-subject voxel-based statistical testing of brain FDG-PET

Brain FDG-PET images of 30 independent ADNI HC subjects were used as normal database (NDB) for voxel-based statistical testing (74.1 ± 3.8 year, 50.0% females).

In preparation for voxel-based testing, all stereotactically normalized and scaled images were smoothed to a spatial resolution of 12 mm full width at half maximum (FWHM).[27,34]

Single-subject analysis was performed separately for each PSP patient and each HC subject by voxel-based statistical testing of the individual FDG-PET image against the NDB using the two-sample t-test model implemented in SPM. Age was taken into account as nuisance covariate.[47,48] Single subjects were tested for both hypometabolism and hypermetabolism using a sensitive significance threshold of $P \le 0.01$ uncorrected for multiple testing.[47,49]

TABLE 1 *Demographic and clinical characteristics*

Characteristic	All PSP patients (n = 41)	PSP-RS (n = 21)	vPSP (n = 20)	Cortical vPSP (n = 11)	Subcortical vPSP (n = 9)	Healthy controls (n = 46)
Age at PET (years)	69.6 ± 7.8 (53.5–81.2)	69.5 ± 7.3 (53.8–81.1)	69.8 ± 8.5 (53.5–81.2)	68.4 ± 8.0 (53.5–79.9)	71.5 ± 9.2 (57.3–81.2)	72.2 ± 4.7 (59.8–79.9)
Sex (% females)	48.8	47.6	50.0	63.6	33.3	39.1
Disease duration at PET (years)	3.1 ± 2.6 (0.4–12.2)	3.1 ± 3.1 (0.4–12.2)	3.0 ± 2.0 (0.4–6.8)	2.5 ± 1.4 (0.8–5.0)	3.7 ± 2.5 (0.4–6.8)	–
Certainty of PSP diagnosis (probable/possible/suggestive of)	35/1/5	21/0/0[a]	14/1/5[a]	9/0/2	5/1/3	–
PSPrs	29.8 ± 14.1 (9–86)	35.1 ± 15.9[a] (15–86)	24.3 ± 9.5[a] (9–47)	26.3 ± 11.4 (9–47)	21.9 ± 6.4 (14–31)	–
MoCA	21.4 ± 4.4 (10–29, n = 32)	20.9 ± 4.2 (11–29, n = 17)	21.9 ± 4.7 (10–28, n = 15)	19.0 ± 5.1[b] (10–24, n = 6)	23.9 ± 3.3[b] (19–28)	–
GDS-15	5.7 ± 2.6 (1–12, n = 28)	5.1 ± 2.5 (1–10, n = 14)	6.2 ± 2.7 (3–12, n = 14)	7.1 ± 3.1 (3–12, n = 7)	5.3 ± 2.0 (3–9, n = 7)	–

Note: The metric parameters were compared (i) between all PSP patients and healthy controls, (ii) between PSP-RS and vPSP, and (iii) between cortical vPSP and subcortical vPSP, using the homo– or heteroscedastic unpaired t-test depending on the result of Levene's test of homogeneity of variance. Sex distribution and certainty of the PSP diagnosis were compared between groups using the chi-square test. Statistically significant effects (two-sided $P \leq 0.05$) are indicated by bold type. If a parameter was not available in all subjects, the number of subjects for that parameter is given in parentheses.

Abbreviations: PSP, progressive supranuclear palsy; PSP-RS, PSP patients with Richardson's syndrome; vPSP, (non-RS) variant PSP; PET, positron emission tomography; PSPrs, PSP rating scale[41]; MoCA, Montreal Cognitive Assessment Scale[42]; GDS-15, 15 points Geriatric Depression Scale.[43]

[a]PSP-RS vs. vPSP $P < 0.05$.
[b]Cortical vPSP vs. subcortical vPSP $P < 0.05$.

Visual interpretation of FDG-PET

Visual interpretation of the FDG-PET images was based on a standardized display provided to the readers as a two-page pdf-document, a separate pdf-document for each subject (Fig. 1, Supplementary Figure S2 in Appendix S1).

The randomly pseudonymized pdf-documents were independently assessed by five readers from four sites (G.B., H.B., I.A., M.B., R.B.) experienced in reading brain FDG-PET with voxel-based testing in patients with suspicion of a neurodegenerative parkinsonian syndrome.

The readers were asked to first score the regional FDG-uptake in the following 12 PSP-related brain regions using a 3-score method (0 = "normal", 1="mildly or moderately reduced", 2 = "strongly reduced"):[26,36] medial frontal cortex (including the anterior cingulate cortex), dorsolateral frontal cortex, anterior insular cortex, caudate nucleus, thalamus, and midbrain, separately in left/right hemisphere. The readers then provided a dichotomic summary assessment as either "PSP patient" or "healthy control".

To support the visual interpretation, a figure showing normal FDG-uptake and normal variability of FDG-uptake in the brain was provided to the readers (Supplementary Fig. S3 in Appendix S1). For the typical brain FDG-PET patterns of different PSP predominance types, the readers were referred to Martí-Andrés et al.[36] No further instructions were given to the readers. The readers were blinded for all clinical data except sex and age.

The readers repeated the reading session with an independent randomization of the pdf-documents to assess intra-reader variability. Mean time interval between the two reading sessions was 23 ± 7 weeks (range 14–34 weeks).

Automatic covariance pattern expression analysis

The expression of the "North American" PSP-related pattern (PSPRP)[50] in individual FDG-PET images was obtained using the voxel-based topographic profile rating method[51-54] implemented in the Scan Analysis and Visualization Processor software package (version ScAnVP7.0w).[53-55] This software package is freely available from the Functional Brain Imaging Laboratory – Center for Neurosciences, Feinstein Institute for Medical Research, Northwell Health (feinsteinneuroscience.org/imaging-software/download-software).

Statistical analyses

Cross tables and the percentage of discrepant cases were used to characterize intra- and between-reader variability as well as the accuracy of the visual

interpretation, separately for each reader or each pair of readers or the majority read.

Pearson's correlation analysis in the independent NDB was used to test PSPRP expression for an impact of healthy aging. Adjustment for age of PSPRP expression was performed by computing residuals with respect to the linear regression of PSPRP expression versus age in the NDB. The age-adjusted residuals of PSPRP expression were transformed to z-scores with respect to mean and standard deviation in the NDB.

Receiver operating characteristic (ROC) analysis was used to characterize the performance of the age-adjusted PSPRP z-score regarding the detection of PSP. The cut-off for dichotomization was derived from the ROC curve according to Youden's criterion.[56]

Statistical analyses were performed with IBM SPSS (version 27). An effect was considered significant if two-sided $P \leq 0.05$.

Results

Twenty-one of the 41 PSP patients (51%) were diagnosed with PSP-RS (Table 1). Among the 20 patients (49%) with vPSP, 11 patients presented with "cortical" vPSP (10 PSP-CBS, 1 PSP-F) and the remaining 9 with "subcortical" vPSP (8 PSP-P, 1 PSP-PGF). A summary of the affected clinical domains is given in Supplementary Table S1 in Appendix S1.

Figure 2 shows the percentage of intra- and between-reader discrepant cases in the visual interpretation in the whole cohort (n = 87), separately for each reader and for each pair of readers. The mean percentage of intra-reader discrepant cases across the five readers was $12.6 \pm 5.8\%$ (range 7–20%). The mean percentage of between-reader discrepant cases across the 10 pairs of readers and the two reading sessions was $21.4 \pm 6.0\%$ (11–34%).

The percentage of intra- and between-reader discrepant cases according to subgroup is also shown in Figure 2.

Mean overall accuracy, sensitivity, specificity, and balanced accuracy of the visual interpretation for the detection of PSP in the whole sample were $70.3\% \pm 6.2\%$, $71.3\% \pm 9.6\%$, $69.3\% \pm 8.4\%$, and $70.3\% \pm 6.3\%$, respectively (mean ± standard deviation [SD] of the five readers and the two reading sessions). Overall accuracy, sensitivity, specificity, and balanced accuracy of the majority visual read were $72.8\% \pm 4.3\%$, $74.0\% \pm 9.2\%$, $71.7\% \pm 0.0\%$, and $72.9\% \pm 4.6\%$, respectively (mean ± SD of the two reading sessions, Fig. 3). Sensitivity and specificity for each individual reader are shown in Supplementary Figure S4.

The percentage of cases misclassified by the majority read according to subgroup is shown in Figure 4.

The PSPRP expression scores increased with age in the NDB (R = 0.374, $P = 0.042$; Supplementary Fig. S5 in Appendix S1) and, therefore, were transformed to age-adjusted z-scores.

In the PSP patients, the age-adjusted PSPRP expression z-score was positively correlated with the PSP rating scale (Spearman correlation coefficient = 0.380, $P = 0.014$). It was not significantly correlated with the Montreal Cognitive Assessment scale ($P = 0.281$), the Geriatric Depression Scale ($P = 0.393$), and disease duration ($P = 0.188$).

The subgroups (PSP-RS, cortical vPSP, subcortical vPSP, HC) explained 45.5% of the between-subject variability of the age-adjusted PSPRP expression z-score (ANOVA-$P < 0.0005$). Compared to the HC group (z-score = 0.17 ± 1.39), the age-adjusted PSPRP expression z-score was significantly increased in all PSP subgroups (PSP-RS: z-score = 3.75 ± 1.72, Scheffé post-hoc test $P < 0.0005$; cortical vPSP: 2.51 ± 2.54, $P = 0.002$; subcortical vPSP: z-score = 2.55 ± 2.17, $P = 0.004$; Fig. 4). Pair-wise differences between PSP subgroups were not significant ($P \geq 0.300$).

The area under the ROC curve of the age-adjusted PSPRP expression z-score for detection of PSP independent of the predominance type was 0.894 (standard error 0.035). It was 0.952 (0.023) when restricted to PSP-RS, 0.834 (0.055) for all vPSP, 0.812 (0.075) for cortical vPSP, and 0.860 (0.060) for subcortical vPSP.

The cut-off 0.89 on the age-adjusted PSPRP expression z-score achieved overall accuracy, sensitivity, specificity, and balanced accuracy of 87.4%, 92.7%, 82.6%, and 87.6%, respectively. When the ROC analysis was restricted to PSP-RS, the Youden criterion resulted in a slightly larger cut-off (1.19) on the z-score.

Discussion

Between-reader variability of the visual interpretation of brain FDG-PET was rather large, although all readers were experienced in FDG-PET reading in suspected PSP. Intra-reader variability was smaller than between-reader variability, but still sizeable. Thus, a considerable fraction of the between-reader variability can be explained by intra-reader variability, indicating that visual reading of brain FDG-PET for the detection of PSP is difficult, even when supported by voxel-based testing. This is in line with previous studies that reported lower accuracy of non-expert readers than expert readers regarding the detection of PSP in FDG-PET,[47] and lower accuracy and confidence of expert readers for the detection of PSP compared to the detection of Parkinson's disease or multiple system atrophy.[47] Intra-reader and between-reader stability were considerably better in PSP-RS compared to vPSP. Among the patients with vPSP, intra-reader variability
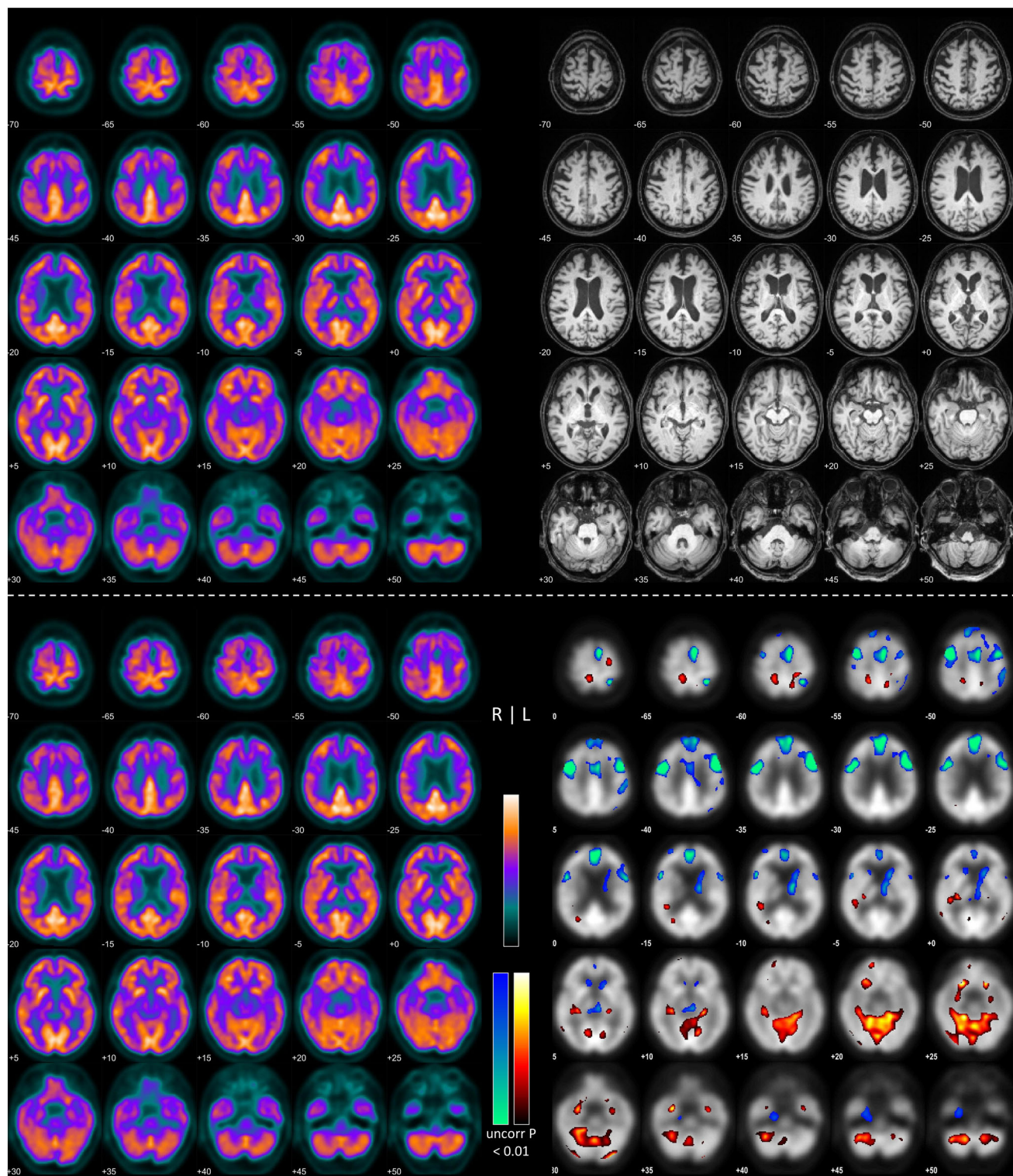
FIG. 1. Standardized display for visual reading of ^{18}F-fluorodeoxyglucose-positron emission tomography (FDG-PET). The upper and lower parts were provided as page 1 and page 2 of a two-page pdf-document, a separate pdf-document for each subject. On each page, the left side shows the subject's stereotactically normalized FDG-uptake image. On page 1, the right side shows the patient's T1w-MRI after mapping to the anatomical reference space using the PET-based transformation. The right side of page 2 shows the parametric maps of hypometabolism ("winter" color table) and hypermetabolism ("hot" color table) from voxel-based statistical testing overlaid to the subject's FDG-PET. The example images shown here are from a 72-year-old woman with diagnosis of probable progressive supranuclear palsy with Richardson's syndrome (PSP-RS). Example images from a healthy control (HC) subject are shown in Supplementary Figure S2 in Appendix S1. vPSP, (non-RS) variant PSP. [Color figure can be viewed at wileyonlinelibrary.com]

FIG. 2. Top: Percentage of intra- and between-reader discrepant cases in the visual interpretation of brain ^{18}F-fluorodeoxyglucose-positron emission tomography (FDG-PET) in the whole sample (n = 87), separately for each of the five readers (R1, …, R5) and for each of the 10 pairs of two readers. For between-reader agreement, mean value and standard deviation (SD) were computed across the two reading sessions. **Bottom:** Percentage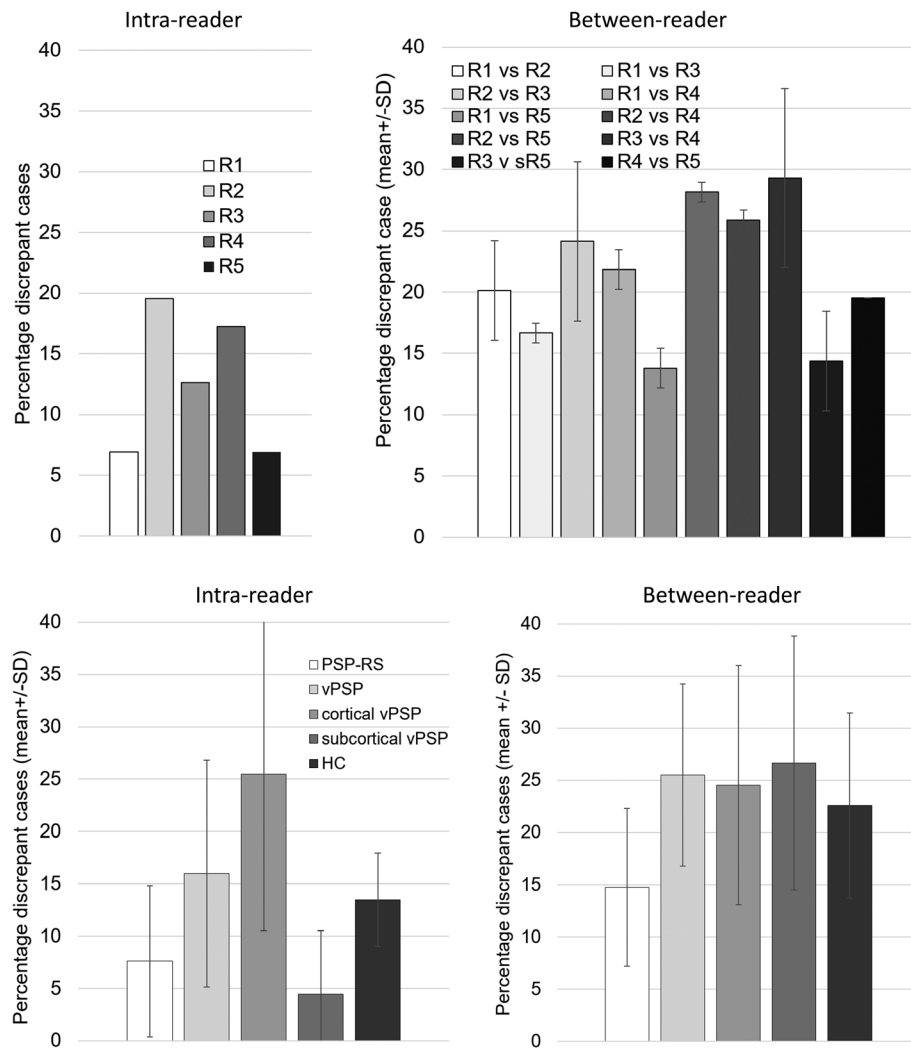 of intra- and between-reader discrepant cases in the visual interpretation according to subgroup. For intra-reader agreement, mean value and SD were computed across the five readers. For between-reader agreement, mean value and SD were computed across the 10 pairs of readers and the two reading sessions. PSP-RS, progressive supranuclear palsy with Richardson's syndrome; vPSP, (non-RS) variant PSP; HC, healthy control.

was larger for cortical vPSP than for subcortical vPSP. Potential explanations include a higher level of attention of the readers during the first reading session that resulted in increased sensitivity for the detection of cortical vPSP but not subcortical vPSP (Supplementary Figs. S6 and S7 in Appendix S1). This suggests that the sensitivity of visual reading might be higher for cortical vPSP than for subcortical vPSP if the reading is performed particularly carefully.

In the whole cohort, visual interpretation of FDG-PET showed balanced sensitivity and specificity only slightly above 70%, lower than reported previously.[49] This is most likely explained by the larger proportion of vPSP in the current study. In fact, the proportion of false-negative cases was about four times larger for vPSP ($\approx$40%) than for PSP-RS ($\approx$10%), in line with the

first hypothesis of this study. Reduced sensitivity of the visual interpretation of FDG-PET for the detection of vPSP probably is related to the fact that the metabolic alterations are often spatially less extended and milder in vPSP than in PSP-RS ("incomplete patterns").[26,34-38] This might also explain reduced specificity, since it increases the risk to misinterpret mild unspecific reduction of FDG-uptake in one of the PSP-characteristic brain regions as indication of vPSP. Retrospective inspection of the PET images of HC subjects misclassified as PSP identified frontal widening of the longitudinal fissure as a major source of false-positive PET interpretation (Supplementary Fig. S8 in Appendix S1).

Only very few studies on FDG-PET in parkinsonian syndromes based the interpretation on visual inspection
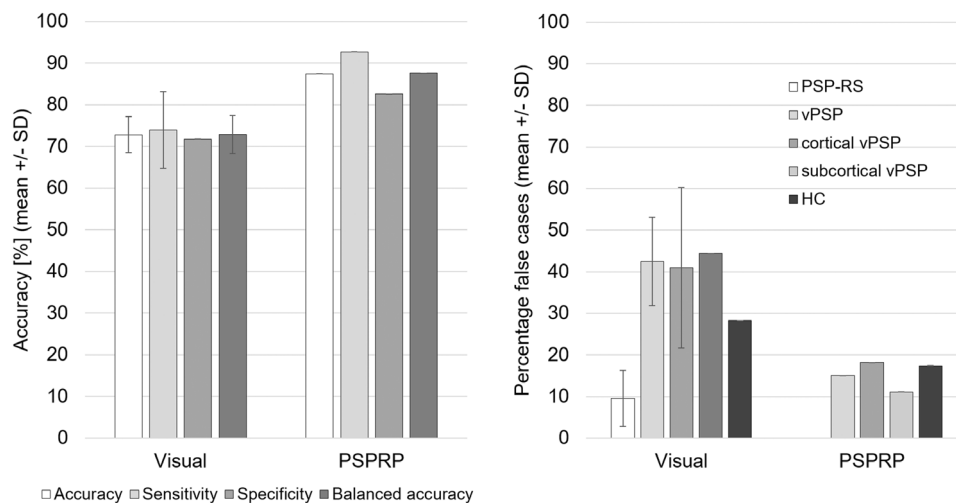
FIG. 3. Accuracy of the majority visual read of the five readers and of the age-adjusted progressive supranuclear palsy-related pattern (PSPRP) expression z-score for the detection of PSP in the whole sample (left), and percentage of misclassified cases by the majority visual read and by the age-adjusted PSPRP expression z-score according to PSP predominance type (right). Mean values and standard deviations (SD) for the majority visual read were computed across the two reading sessions. For the age-adjusted PSPRP expression z-score, the cut-off derived from the receiver operating characteristic (ROC) curve in the whole sample was used. PSP-RS, progressive supranuclear palsy with Richardson's syndrome; vPSP, (non-RS) variant PSP; HC, healthy control.

of the FDG-uptake images alone.[29] Here, visual FDG-PET reading was supported by voxel-based statistical testing as in most previous studies.[38,48,49,57-69] Voxel-based testing increases reader confidence[47] and accuracy of FDG-PET in parkinsonian syndromes,[47,49,60] particularly in less experienced readers.[47] Procedure guidelines recommend supporting visual FDG-PET analysis with observer-independent approaches such as voxel-based statistical testing "especially for less-skilled readers and, more generally, with the aim to reduce inter-reader variability".[70,71] Thus, the visual PET reading in this study was in line with current guidelines, and it represents clinical practice at most sites.

However, statistical maps have to be interpreted by the user. Thus, voxel-based testing does not fully eliminate intra- and between-reader variability in brain FDG-PET.[50] Furthermore, voxel-based testing has only limited sensitivity to capture functional interactions among brain regions. It applies the same univariate test and the same significance threshold at each image voxel. Potentially relevant information is missed when it does not reach the predefined significance threshold. Furthermore, intensity scaling of FDG-uptake images for voxel-based testing results in reduced sensitivity for the detection of regional hypometabolism if the reference region for intensity scaling is affected by disease-
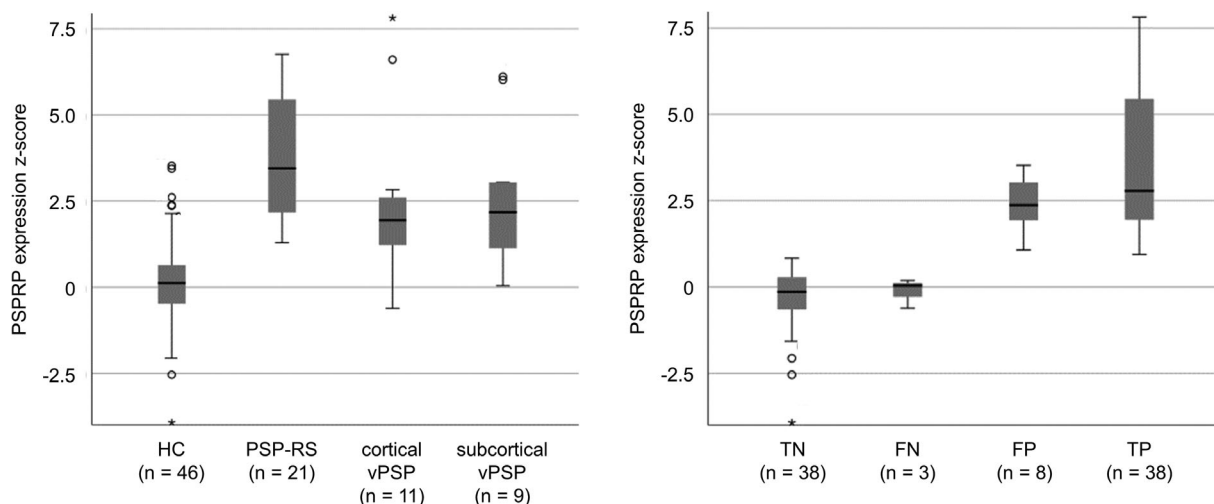
FIG. 4. Age-adjusted progressive supranuclear palsy-related pattern (PSPRP) expression z-score in the different subgroups (left) and versus classification based on the cut-off derived from receiver operating characteristic (ROC) analysis in the whole sample. HC, healthy control; PSP-RS, progressive supranuclear palsy with Richardson's syndrome; vPSP, (non-RS) variant PSP; TN, true-negative; FN, false-negative; FP, false-positive; TP, true-positive.

related hypometabolism.[72,73] Tracer kinetic modeling to estimate the regional metabolic rate of glucose (in milligram glucose per gram tissue per minute) eliminates the need for intensity scaling.[15-18,20,35,74] However, kinetic modeling requires measurement of the time course of FDG in arterial plasma ("input function") by drawing arterial blood samples.[75] This is not feasible for all patients in clinical practice, even though the input function might be obtained by sampling "arterialized" venous blood.[76]

Limitations of voxel-based testing are overcome by covariance pattern analysis using scaled subprofile model principal component analysis (SSM-PCA) to identify disease-related patterns.[51,53,77,78] Disease-related covariance patterns more likely cover the full spatial extent of metabolic changes throughout the whole brain than statistical maps from univariate voxel-based testing. Once the disease-related pattern has been identified in a training set, its expression can be computed for new FDG-PET images. The computation is fully automatic and, therefore, user-independent. Covariance pattern analysis does not require intensity scaling and, therefore, is not affected by limitations of a reference region.

Automatic quantification of the expression of disease-related patterns was validated for the (differential) diagnosis of neurodegenerative parkinsonian syndromes in numerous studies.[30-32,36,37,50,58,79-87] It provides high accuracy for the detection of PSP also at early clinical stages.[80]

Covariance pattern analysis is robust with respect to image variability associated with different scanner hardware and/or software.[55] In particular, the PSPRP is highly consistent across populations and PET scanners (Supplementary Fig. S9 in Appendix S1).[32,36,37,58,79,88] This is an important prerequisite for widespread clinical use. In particular, it allows sharing of disease-related patterns between sites. The current study used the "North American" PSPRP derived about 15 years ago[50] and validated in independent cohorts from North America,[80,89] Europe,[30] South Korea,[37] and India.[82]

A novel finding of this study was the significant decline of PSPRP expression with healthy aging, suggesting that age adjustment is required to optimize the diagnostic performance of PSPRP expression analysis. The area under the ROC curve for detection of PSP was significantly ($P = 0.008$) smaller without than with age adjustment (data not shown).

In the whole cohort, PSPRP expression analysis clearly outperformed visual interpretation with respect to both sensitivity and specificity. The improvement was not restricted to PSP-RS. On the contrary, sensitivity improvement was even more pronounced in vPSP, supporting the second hypothesis of the study. This suggests that PSPRP expression analysis provides clinically useful discriminative power also in non-RS PSP, in line with a previous study that included 36% vPSP patients.[36]

The North American PSPRP was derived from 10 patients with PSP according to the NINDS criteria that probably overrepresented PSP-RS.[50] The current study made no attempts to adapt the North American PSPRP to the current PSP sample in order to avoid overly optimistic performance estimates due to overfitting. The FDG-PET images of the PSP patients were obtained retrospectively from multiple sites without specific eligibility criteria. In particular, no cases were excluded due to limited PET image quality. Thus, the current performance estimates should be representative of covariance pattern analysis with the North American PSPRP in clinical practice at most sites.

Age-adjusted PSPRP expression was slightly higher in false-negative compared to true-negative cases and slightly lower in false-positive compared to true-positive cases (Fig. 4). This suggests that the PSPRP expression score might contribute to the characterization of the confidence of the automatic interpretation beyond binary classification.

In a study on covariance pattern analysis, PSPRP expression discriminated PSP-RS and PSP-P patients from healthy controls.[36] PSP-PGF also showed elevated PSPRP expression, but the effect did not reach statistical significance.[36] The authors concluded that "… despite the existence of probable neuropathological and functional differences between PSP variants, they may also share a common pattern that can serve as a PSP biomarker…". Another FDG-PET study found no significant difference in PSPRP expression between PSP-RS and PSP-P.[37] The authors concluded that "a common generic disease network is expressed by patients with the disorder, irrespective of clinical presentation".[37] In another study, 5 patients with corticobasal syndrome and neuropathological PSP diagnosis presented the typical PSP pattern in FDG-PET.[27] Thus, FDG-PET does not simply mirror symptoms, but reveals metabolic alterations that are associated with the pathology.[27,90] This is the basis for FDG-PET to support the etiological diagnosis of neurodegenerative parkinsonian syndromes.

Differences in PSPRP expression between PSP predominance types suggest that the sensitivity of automatic covariance analysis for the detection of non-RS predominance types might be improved by adding type-specific patterns (Supplementary Fig. S9 in Appendix S1).

Disease-characteristic FDG-PET indices derived by deep machine learning showed promising performance regarding (differential) diagnosis of neurodegenerative parkinsonian syndromes.[91,92] Further validation is required to recommended these indices for clinical use.

The following limitations of this study should be noted. First, the number of PSP patients was rather small. This is explained by the fact that inclusion was restricted to PET examinations from PET systems that were still available for a Hoffman 3D phantom measurement for retrospective harmonization of spatial resolution.

Second, the clinical PSP diagnosis was obtained close in time to PET. Verification of the diagnosis was not available, neither by neuropathology nor by follow-up. Thus, limitations of the clinical diagnosis at early disease stages[8] and with respect to the allocation of PSP patients to a specific predominance type[93] should be taken into account.

Third, the clinical diagnosis was made after FDG-PET in 24 of the 41 PSP patients (58.5%) and was not blinded for the FDG-PET finding. This might have caused a selection bias in favor of FDG-PET. This mainly affects the sensitivity of FDG-PET for the detection of PSP-RS, since the clinical diagnosis was made after FDG-PET in 17 of the 21 PSP-RS patients (81%). The proportion of cases in which the clinical diagnosis was made after PET was considerably smaller among the vPSP patients (7 of 20, 35%), so that the sensitivity estimates for the detection of vPSP should be less affected. Furthermore, the potential selection bias probably did not favor PSPRP expression analysis over visual image interpretation, since none of the participating sites performed PSPRP expression analysis at the time of FDG-PET. The cut-off on the age-adjusted PSPRP expression z-score to compute sensitivity and specificity was derived in the same sample to which it was applied, which might have caused a bias. Potential limitations associated with the cut-off do not affect the area under the ROC curve.

Fourth, the study was restricted to the detection of PSP. The differentiation of PSP from other neurodegenerative parkinsonian syndromes was not assessed.

Finally, no attempts were made to differentiate between PSP predominance types based on FDG-PET. The rationale was that the syndromic characterization is part of the clinical assessment. FDG-PET is used to support the etiological diagnosis of the underlying pathology independent of the clinical phenotype.

In conclusion, visual interpretation of brain FDG-PET supported by voxel-based testing provides good accuracy for the detection of PSP-RS, but only fair sensitivity for the detection of vPSP predominance types. Automatic covariance pattern expression analysis outperforms visual interpretation with respect to the detection of PSP-RS, provides clinically useful sensitivity also for the detection of vPSP, and reduces the rate of false-positive findings. We recommend the use of pattern expression analysis to complement visual reading and voxel-based testing of brain FDG-PET in suspected PSP. ▪

Ethical Statement

We confirm that we have read the Journal's position on issues involved in ethical publication and affirm that this work is consistent with those guidelines. Waiver of informed consent for the retrospective analyses of this study was obtained from the relevant ethics review boards.

Data Availability Statement

Visual and PSPRP expression scores are available from the corresponding author.

References

1. Stamelou M, Respondek G, Giagkou N, Whitwell JL, Kovacs GG, Hoglinger GU. Evolving concepts in progressive supranuclear palsy and other 4-repeat tauopathies. Nat Rev Neurol 2021;17(10):601–620.

2. Roemer SF, Grinberg LT, Crary JF, et al. Rainwater Charitable Foundation criteria for the neuropathologic diagnosis of progressive supranuclear palsy. Acta Neuropathol 2022;144(4):603–614.

3. Litvan I, Agid Y, Calne D, et al. Clinical research criteria for the diagnosis of progressive supranuclear palsy (Steele-Richardson-Olszewski syndrome): report of the NINDS-SPSP International Workshop. Neurology 1996;47(1):1–9.

4. Respondek G, Roeber S, Kretzschmar H, et al. Accuracy of the National Institute for Neurological Disorders and Stroke/Society for Progressive Supranuclear Palsy and Neuroprotection and Natural History in Parkinson Plus Syndromes criteria for the diagnosis of progressive supranuclear palsy. Mov Disord 2013;28(4):504–509.

5. Hoglinger GU, Respondek G, Stamelou M, et al. Clinical diagnosis of progressive supranuclear palsy: the Movement Disorder Society criteria. Mov Disord 2017;32(6):853–864.

6. Respondek G, Stamelou M, Kurz C, et al. The phenotypic spectrum of progressive supranuclear palsy: a retrospective multicenter study of 100 definite cases. Mov Disord 2014;29(14):1758–1766.

7. Jabbari E, Holland N, Chelban V, et al. Diagnosis across the spectrum of progressive supranuclear palsy and corticobasal syndrome. JAMA Neurol 2020;77(3):377–387.

8. Ali F, Martin PR, Botha H, et al. Sensitivity and specificity of diagnostic criteria for progressive supranuclear palsy. Mov Disord 2019; 34(8):1144–1153.

9. van Eimeren T, Antonini A, Berg D, et al. Neuroimaging biomarkers for clinical trials in atypical parkinsonian disorders: proposal for a neuroimaging biomarker utility system. Alzheimers Dement (Amst) 2019;11:301–309.

10. Saeed U, Lang AE, Masellis M. Neuroimaging advances in Parkinson's disease and atypical parkinsonian syndromes. Front Neurol 2020;11:572976.

11. Whitwell JL, Holinger GU, Antonini A, et al. Radiological biomarkers for diagnosis in PSP: where are we and where do we need to be? Mov Disord 2017;32(7):955–971.

12. Meyer PT, Frings L, Rucker G, Hellwig S. (18)F-FDG PET in parkinsonism: differential diagnosis and evaluation of cognitive impairment. J Nucl Med 2017;58(12):1888–1898.

13. Brooks DJ. Imaging of genetic and degenerative disorders primarily causing parkinsonism. Handb Clin Neurol 2016;135:493–505.

14. Sokoloff L. Energetics of functional activation in neural tissues. Neurochem Res 1999;24(2):321–329.

15. D'Antona R, Baron JC, Samson Y, et al. Subcortical dementia. Frontal cortex hypometabolism detected by positron tomography in patients with progressive supranuclear palsy. Brain 1985;108(Pt 3): 785–799.

16. Foster NL, Gilman S, Berent S, Morin EM, Brown MB, Koeppe RA. Cerebral hypometabolism in progressive supranuclear palsy studied with positron emission tomography. Ann Neurol 1988;24(3): 399–406.

17. Blin J, Baron JC, Dubois B, et al. Positron emission tomography study in progressive supranuclear palsy – brain hypometabolic pattern and clinicometabolic correlations. Arch Neurol 1990;47(7): 747–752.

18. Goffinet AM, Devolder AG, Gillain C, et al. Positron tomography demonstrates frontal-lobe hypometabolism in progressive supranuclear palsy. Ann Neurol 1989;25(2):131–139.

19. Otsuka M, Ichiya Y, Kuwabara Y, et al. Cerebral blood flow, oxygen and glucose metabolism with PET in progressive supranuclear palsy. Ann Nucl Med 1989;3(3):111–118.

20. Karbe H, Grond M, Huber M, Herholz K, Kessler J, Heiss WD. Subcortical damage and cortical dysfunction in progressive supranuclear palsy demonstrated by positron emission tomography. J Neurol 1992;239(2):98–102.

21. Leenders KL, Frackowiak RSJ, Lees AJ. Steele-Richardson-Olszewski syndrome – brain energy-metabolism, blood-flow and fluorodopa uptake measured by positron emission tomography. Brain 1988;111:615–630.

22. Botha H, Whitwell JL, Madhaven A, Senjem ML, Lowe V, Josephs KA. The pimple sign of progressive supranuclear palsy syndrome. Parkinsonism Relat Disord 2014;20(2):180–185.

23. Niccolini F, Politis M. A systematic review of lessons learned from PET molecular imaging research in atypical parkinsonism. Eur J Nucl Med Mol Imaging 2016;43(12):2244–2254.

24. Berti V, Pupi A, Mosconi L. PET/CT in diagnosis of movement disorders. Ann N Y Acad Sci 2011;1228:93–108.

25. Buchert R, Buhmann C, Apostolova I, Meyer PT, Gallinat J. Nuclear imaging in the diagnosis of clinically uncertain parkinsonian syndromes. Dtsch Arztebl Int 2019;116(44):747–754.

26. Zalewski N, Botha H, Whitwell JL, Lowe V, Dickson DW, Josephs KA. FDG-PET in pathologically confirmed spontaneous 4R-tauopathy variants. J Neurol 2014;261(4):710–716.

27. Pardini M, Huey ED, Spina S, et al. FDG-PET patterns associated with underlying pathology in corticobasal syndrome. Neurology 2019;92(10):E1121–E1135.

28. Smith R, Scholl M, Honer M, Nilsson CF, Englund E, Hansson O. Tau neuropathology correlates with FDG-PET, but not AV-1451-PET, in progressive supranuclear palsy. Acta Neuropathol 2017;133(1):149–151.

29. Oh M, Lee N, Kim C, et al. Diagnostic accuracy of dual-phase (18) F-FP-CIT PET imaging for detection and differential diagnosis of parkinsonism. Sci Rep 2021;11(1):14992.

30. Rus T, Tomse P, Jensterle L, et al. Differential diagnosis of parkinsonian syndromes: a comparison of clinical and automated – metabolic brain patterns' based approach. Eur J Nucl Med Mol Imaging 2020;47(12):2901–2910.

31. Shen B, Wei S, Ge J, et al. Reproducible metabolic topographies associated with multiple system atrophy: network and regional analyses in Chinese and American patient cohorts. Neuroimage Clin 2020;28:102416.

32. Tomse P, Rebec E, Studen A, et al. Abnormal metabolic covariance patterns associated with multiple system atrophy and progressive supranuclear palsy. Phys Med 2022;98:131–138.

33. Dickson DW, Ahmed Z, Algom AA, Tsuboi Y, Josephs KA. Neuropathology of variants of progressive supranuclear palsy. Curr Opin Neurol 2010;23(4):394–400.

34. Park HK, Kim JS, Im KC, et al. Functional brain imaging in pure akinesia with gait freezing: [18F] FDG PET and [18F] FP-CIT PET analyses. Mov Disord 2009;24(2):237–245.

35. Taniwaki T, Hosokawa S, Goto I, et al. Positron emission tomography (PET) in pure akinesia. J Neurol Sci 1992;107(1):34–39.

36. Martí-Andrés G, van Bommel L, Meles SK, et al. Multicenter validation of metabolic abnormalities related to PSP according to the MDS-PSP criteria. Mov Disord 2020;35(11):2009–2018.

37. Ko JH, Lee CS, Eidelberg D. Metabolic network expression in parkinsonism: clinical and dopaminergic correlations. J Cereb Blood Flow Metab 2017;37(2):683–693.

38. Srulijes K, Reimold M, Liscic RM, et al. Fluorodeoxyglucose positron emission tomography in Richardson's syndrome and progressive supranuclear palsy-parkinsonism. Mov Disord 2012;27(1): 151–155.

39. Garibotto V, Herholz K, Boccardi M, et al. Clinical validity of brain fluorodeoxyglucose positron emission tomography as a biomarker for Alzheimer's disease in the context of a structured 5-phase development framework. Neurobiol Aging 2017;52:183–195.

40. Fazekas F, Chawluk JB, Alavi A, Hurtig HI, Zimmerman RA. MR signal abnormalities at 1.5 T in Alzheimer's dementia and normal aging. AJR Am J Roentgenol 1987;149(2):351–356.

41. Golbe LI, Ohman-Strickland PA. A clinical rating scale for progressive supranuclear palsy. Brain 2007;130:1552–1565.

42. Nasreddine ZS, Phillips NA, Bedirian V, et al. The Montreal Cognitive Assessment, MoCA: a brief screening tool for mild cognitive impairment. J Am Geriatr Soc 2005;53(4):695–699.

43. Sheikh JI, Yesavage JA. Geriatric Depression Scale (GDS): recent evidence and development of a shorter version. Clin Gerontol 1986;5: 165–173.

44. Hoffman EJ, Cutler PD, Digby WM, Mazziotta JC. 3-D phantom to simulate cerebral blood-flow and metabolic images for PET. IEEE Trans Nucl Sci 1990;37(2):616–620.

45. Statistical Parametric Mapping. The Analysis of Functional Brain Images. London: Academic Press; 2006.

46. Brumberg J, Schroter N, Blazhenets G, et al. Differential diagnosis of parkinsonism: a head-to-head comparison of FDG PET and MIBG scintigraphy. NPJ Parkinsons Dis 2020;6(1):39.

47. Arnone A, Allocca M, Di Dato R, et al. FDG PET in the differential diagnosis of degenerative parkinsonian disorders: usefulness of voxel-based analysis in clinical practice. Neurol Sci 2022;43(9): 5333–5341.

48. Mishina M, Ishii K, Mitani K, et al. Midbrain hypometabolism as early diagnostic sign for progressive supranuclear palsy. Acta Neurol Scand 2004;110(2):128–135.

49. Eckert T, Barnes A, Dhawan V, et al. FDG PET in the differential diagnosis of parkinsonian disorders. Neuroimage 2005;26(3): 912–921.

50. Eckert T, Tang CK, Ma YL, et al. Abnormal metabolic networks in atypical parkinsonism. Mov Disord 2008;23(5):727–733.

51. Spetsieris PG, Eidelberg D. Scaled subprofile modeling of resting state imaging data in Parkinson's disease: methodological issues. Neuroimage 2011;54(4):2899–2914.

52. Moeller JR, Strother SC, Sidtis JJ, Rottenberg DA. Scaled subprofile model: a statistical approach to the analysis of functional patterns in positron emission tomographic data. J Cereb Blood Flow Metab 1987;7(5):649–658.

53. Spetsieris P, Ma Y, Peng S, et al. Identification of disease-related spatial covariance patterns using neuroimaging data. J Vis Exp 2013; 76:e50319.

54. Eidelberg D. Metabolic brain networks in neurodegenerative disorders: a functional imaging approach. Trends Neurosci 2009;32(10): 548–557.

55. Peng S, Ma Y, Spetsieris PG, et al. Characterization of disease-related covariance topographies with SSMPCA toolbox: effects of spatial normalization and PET scanners. Hum Brain Mapp 2014; 35(5):1801–1814.

56. Youden WJ. Index for rating diagnostic tests. Cancer 1950;3(1): 32–35.

57. Teune LK, Bartels AL, de Jong BM, et al. Typical cerebral metabolic patterns in neurodegenerative brain diseases. Mov Disord 2010; 25(14):2395–2404.

58. Teune LK, Renken RJ, Mudali D, et al. Validation of parkinsonian disease-related metabolic brain patterns. Mov Disord 2013;28(4): 547–551.

59. Juh R, Kim J, Moon D, Choe B, Suh T. Different metabolic patterns analysis of parkinsonism on the 18F-FDG PET. Eur J Radiol 2004; 51(3):223–233.

60. Zhao P, Zhang B, Gao S. 18F-FDG PET study on the idiopathic Parkinson's disease from several parkinsonian-plus syndromes. Parkinsonism Relat Disord 2012;18(Suppl. 1):S60–S62.

61. Hosaka K, Ishii K, Sakamoto S, et al. Voxel-based comparison of regional cerebral glucose metabolism between PSP and corticobasal degeneration. J Neurol Sci 2002;199(1–2):67–71.

62. Garraux G, Salmon E, Peigneux P, et al. Voxel-based distribution of metabolic impairment in corticobasal degeneration. Mov Disord 2000;15(5):894–904.

63. Klein RC, de Jong BM, de Vries JJ, Leenders KL. Direct comparison between regional cerebral metabolism in progressive supranuclear palsy and Parkinson's disease. Mov Disord 2005;20(8):1021–1030.

64. Salmon E, Van der Linden MV, Franck G. Anterior cingulate and motor network metabolic impairment in progressive supranuclear palsy. Neuroimage 1997;5(3):173–178.

65. Zhao P, Zhang B, Gao S, Li X. Clinical, MRI and 18F-FDG-PET/CT analysis of progressive supranuclear palsy. J Clin Neurosci 2020;80:318–323.

66. Hellwig S, Amtage F, Kreft A, et al. [F-18]FDG-PET is superior to [I-123]IBZM-SPECT for the differential diagnosis of parkinsonism. Neurology 2012;79(13):1314–1322.

67. Caminiti SP, Alongi P, Majno L, et al. Evaluation of an optimized [F-18]fluoro-deoxy-glucose positron emission tomography voxel-wise method to early support differential diagnosis in atypical parkinsonian disorders. Eur J Neurol 2017;24(5):687.

68. Tripathi M, Dhawan V, Peng SC, et al. Differential diagnosis of parkinsonian syndromes using F-18 fluorodeoxyglucose positron emission tomography. Neuroradiology 2013;55(4):483–492.

69. Brajkovic L, Kostic V, Sobic-Saranovic D, et al. The utility of FDG-PET in the differential diagnosis of parkinsonism. Neurol Res 2017; 39(8):675–684.

70. Guedj E, Varrone A, Boellaard R, et al. EANM procedure guidelines for brain PET imaging using [(18)F]FDG, version 3. Eur J Nucl Med Mol Imaging 2022;49(2):632–651.

71. Nobili F, Arbizu J, Bouwman F, et al. European Association of Nuclear Medicine and European Academy of Neurology recommendations for the use of brain (18) F-fluorodeoxyglucose positron emission tomography in neurodegenerative cognitive impairment and dementia: Delphi consensus. Eur J Neurol 2018;25(10):1201–1217.

72. Buchert R, Wilke F, Chakrabarti B, et al. Adjusted scaling of FDG positron emission tomography images for statistical evaluation in patients with suspected Alzheimer's disease. J Neuroimaging 2005; 15(4):348–355.

73. Borghammer P, Cumming P, Aanerud J, Forster S, Gjedde A. Sub-cortical elevation of metabolism in Parkinson's disease – a critical reappraisal in the context of global mean normalization. Neuroimage 2009;47(4):1514–1521.

74. Nagahama Y, Fukuyama H, Turjanski N, et al. Cerebral glucose metabolism in corticobasal degeneration: comparison with progressive supranuclear palsy and normal controls. Mov Disord 1997; 12(5):691–696.

75. Hutchins GD, Holden JE, Koeppe RA, Halama JR, Gatley SJ, Nickles RJ. Alternative approach to single-scan estimation of cerebral glucose metabolic rate using glucose analogs, with particular application to ischemia. J Cereb Blood Flow Metab 1984;4(1): 35–40.

76. Phelps ME, Huang SC, Hoffman EJ, Selin C, Sokoloff L, Kuhl DE. Tomographic measurement of local cerebral glucose metabolic rate in humans with (F-18)2-fluoro-2-deoxy-D-glucose: validation of method. Ann Neurol 1979;6(5):371–388.

77. Niethammer M, Eidelberg D. Metabolic brain networks in translational neurology: concepts and applications. Ann Neurol 2012; 72(5):635–647.

78. Spetsieris PG, Ma Y, Dhawan V, Eidelberg D. Differential diagnosis of parkinsonian syndromes using PCA-based functional imaging features. Neuroimage 2009;45(4):1241–1252.

79. Ge J, Wu J, Peng S, et al. Reproducible network and regional topographies of abnormal glucose metabolism associated with progressive supranuclear palsy: multivariate and univariate analyses in American and Chinese patient cohorts. Hum Brain Mapp 2018;39(7): 2842–2858.

80. Tang CC, Poston KL, Eckert T, et al. Differential diagnosis of parkinsonism: a metabolic imaging study using pattern analysis. Lancet Neurol 2010;9(2):149–158.

81. Garraux G, Phillips C, Schrouff J, et al. Multiclass classification of FDG PET scans for the distinction between Parkinson's disease and atypical parkinsonian syndromes. Neuroimage Clin 2013;2: 883–893.

82. Tripathi M, Tang CC, Feigin A, et al. Automated differential diagnosis of early parkinsonism using metabolic brain networks: a validation study. J Nucl Med 2016;57(1):60–66.

83. Hirano S, Eckert T, Flanagan T, Eidelberg D. Metabolic networks for assessment of therapy and diagnosis in Parkinson's disease. Mov Disord 2009;24(Suppl. 2):S725–S–731.

84. Eidelberg D, Moeller JR, Dhawan V, et al. The metabolic topography of parkinsonism. J Cereb Blood Flow Metab 1994;14(5): 783–801.

85. Ma Y, Tang C, Spetsieris PG, Dhawan V, Eidelberg D. Abnormal metabolic network activity in Parkinson's disease: test-retest reproducibility. J Cereb Blood Flow Metab 2007;27(3):597–605.

86. Niethammer M, Tang CC, Feigin A, et al. A disease-specific metabolic brain network associated with corticobasal degeneration. Brain 2014;137(Pt 11):3036–3046.

87. Papathoma PE, Markaki I, Tang C, et al. A replication study, systematic review and meta-analysis of automated image-based diagnosis in parkinsonism. Sci Rep 2022;12(1):2763.

88. Tomse P, Jensterle L, Rep S, et al. The effect of 18F-FDG-PET image reconstruction algorithms on the expression of characteristic metabolic brain network in Parkinson's disease. Phys Med 2017;41: 129–135.

89. Schindlbeck KA, Gupta DK, Tang CC, et al. Neuropathological correlation supports automated image-based differential diagnosis in parkinsonism. Eur J Nucl Med Mol Imaging 2021;48(11):3522–3529.

90. Cerami C, Dodich A, Iannaccone S, et al. Individual brain metabolic signatures in corticobasal syndrome. J Alzheimers Dis 2020;76(2): 517–528.

91. Wu P, Zhao Y, Wu J, et al. Differential diagnosis of parkinsonism based on deep metabolic imaging indices. J Nucl Med 2022;63(11): 1741–1747.

92. Zhao Y, Cumming P, Rominger A, et al. A 3D deep residual convolutional neural network for differential diagnosis of parkinsonian syndromes on (18)F-FDG PET images. Annu Int Conf IEEE Eng Med Biol Soc 2019;2019:3531–3534.

93. Grimm MJ, Respondek G, Stamelou M, et al. How to apply the Movement Disorder Society criteria for diagnosis of progressive supranuclear palsy. Mov Disord 2019;34(8):1228–1232.

Supporting Data

Additional Supporting Information may be found in the online version of this article at the publisher's web-site.